

## **Supplementary Materials for**

### **Snail-Regulated Exosomal MicroRNA-21 Suppresses NLRP3 Inflammasome Activity to Enhance Cisplatin Resistance**

Han-Ying Cheng, Chia-Hsin Hsieh, Po-Han Lin, Yu-Tung Chen, Dennis Shin-Shian Hsu, Shyh-Kuan Tai, Pen-Yuan Chu, and Muh-Hwa Yang

#### **Supplementary materials include:**

**Supplementary methods with references**

**10 supplementary figures with legends**

**Legends for 14 supplementary tables**

## Supplementary methods

### HNSCC patients

The patient characteristics are presented in the corresponding supplementary tables. The first group comprised nine cases of multiplex immunofluorescence staining (supplementary figure 1A, supplementary table 1). The second group comprised frozen samples of 65 dissected tumors derived from 21 HNSCC patients and contralateral normal oral epithelia (supplementary table 2). Bulk RNA sequencing was performed for tumors and normal samples (figure 1B). The third group included 50 samples and the contralateral normal oral epithelia (supplementary table 3). The relative expression levels of *SNAIL*, miR-21, *CXCL9*, *CXCL10*, and *IFNG* were determined by analyzing the fold changes in the tumor tissues compared with their normal counterparts (figure 7B). The fourth group included 19 HNSCC patients who received chemotherapy at the Taipei Veterans General Hospital. The tumor tissues were subjected to staining with an anti-Snail antibody for the categorization of patients (supplementary table 4). The serum levels of IL-1 $\beta$  before and after chemotherapy were determined before and 1 d after chemotherapy (figure 7C-D). RECIST criteria was applied to define response to chemotherapy<sup>1</sup>. For partial response, at least a 30% decrease in the sum of diameters of target lesions, taking as reference the baseline sum diameter. For progressive disease, at least a 20% increase in the sum of diameters of target lesions, taking as reference the smallest sum on study (this includes the baseline sum if that is the smallest on study). In addition to the relative increase of 20%, the sum must also demonstrate an absolute increase of at least 5 mm. The fifth group comprised six paraffin-embedded samples from HNSCC patients receiving treatment at the Taipei Veterans General Hospital (supplementary table 5). The samples were used for PLA/immunofluorescence staining to determine the NLRP3 inflammasome activity in TAMs (figure 7E).

### RNA-seq analysis of HNSCC patient samples

We used the following two datasets of RNA-seq data derived from HNSCC patients for analysis: TCGA HNSCC (n=521, website: <https://www.cancer.gov/tcga>) and Taipei Veterans General Hospital (TVGH) HNSCC

(21 normal oral epithelia, 35 primary tumors, and 9 metastatic tumors from 21 patients; see supplementary table 2 for the patient characteristics). Data on TCGA HNSCC sequences were downloaded by using Xena<sup>2</sup> and cBioPortal<sup>3</sup> and normalized to Z score or  $\log_2(\text{RPM}+1)$  or  $\log_2(\text{norm\_count}+1)$ . We applied the EMT score to categorize the patients. Briefly, EMT score is defined as the average of Z-score mesenchymal markers (*VIM*, *FNI*, *CDH2*, *ITBG6*, *FOXC2*, *MMP2*, *MMP3*, *MMP9*, *SOX10*, *SNAIL1*, *SNAIL2*, *TWIST1*, *GSC*) / average epithelial marker (*CDH1*, *DSP*, *TJPI*)<sup>4</sup>. We selected and categorized the top one-third EMT score patients as the EMT<sup>high</sup> subgroup (n=172 for TCGA and n=22 for TVGH) and the lowest one-third EMT score patients as the EMT<sup>low</sup> subgroup (n=172 for TCGA and n=22 for TVGH). The expression of the genes of interest was compared in the EMT<sup>high</sup> versus EMT<sup>low</sup> subgroups of TCGA and TVGH HNSCC cases.

### RNA sequencing for exosomal small RNA

For exosomal small RNA sequencing, exosomes were collected, and total RNA extraction was performed. Small RNA fractions were sequenced using the Illumina Genome Analyzer II (Illumina). ConDeTri was used to trim or remove reads according to the quality score. Qualified reads after filtering low-quality data were analyzed using miRDeep2 to clip the 3' adapter sequence, and reads shorter than 18 nucleotides were discarded before performing the alignment of reads to the human and mouse genomes from UCSC. The expression profiles of miRNAs in FaDu exosomes versus SG exosomes are listed in supplementary table 7.

### Preparation of conditional media and macrophages

To produce conditioned media using cancer cells, human HNSCC cell lines FaDu/OECM1 with overexpression or knockdown of Snail were cultured in the RPMI 1640 growth medium supplemented with penicillin/streptomycin and 0.5% FBS for 48 h. The supernatant was centrifuged at  $2,000 \times g$  for 5 min, and was subsequently collected and stored at  $-80^\circ\text{C}$ . To prepare human peripheral blood mononuclear cells (PBMC)-derived macrophages, CD14<sup>+</sup> monocytes were isolated from the whole blood samples obtained from healthy donors and were cultured in the RPMI 1640 medium containing 10% FBS and 20 ng/ml GM-CSF for 5

days. To generate THP-1-derived macrophages, THP-1 cells were subjected to differentiation overnight with 20 ng/ml phorbol 12-myristate 13-acetate. To induce activation of inflammasomes, the cells were primed with 1 µg/ml LPS for 4 h, following by 5 µM nigericin treatment in conditioned media for 1 h. In some experiments, we used 1 µg/ml LPS for 4 h following by 20 ng/ml IFN-γ in conditioned media for 48 h to stimulate PBMC-derived macrophages (supplementary figure 3A and supplementary figure 5A, 5B, 5E, 5F, 5G).

### **Purification and characterization of tumor-derived exosomes**

Exosome purification was performed as per methods described previously<sup>5</sup>. Briefly, exosomes were purified by differential ultracentrifugation. First, the cells were removed from the conditioned medium via centrifugation at  $300 \times g$  for 10 min. To remove large dead cells and substantial cell debris, the supernatants were successively centrifuged at increasing speeds ( $2,000 \times g$  for 10 min,  $10,000 \times g$  for 30 min, the Beckman SW28 rotor). The supernatant was ultracentrifuged at  $100,000 \times g$  for 70 min to pellet the exosomes. Exosomes were subjected to washing steps in PBS and were centrifuged at the same high speed (the Beckman TLA-100.3 rotor). The morphology and size distribution of exosomes were analyzed by performing transmission electron microscopy (JEOL JEM-2000EXII, JEOL USA, Inc., Peabody, MA) and nanoparticle tracking analysis (NanoSight LM10-HS, Malvern Panalytical, Malvern, UK), respectively.

### **Tissue processing and data generation for Visium spatial gene expression**

The sample used for Visium spatial gene expression analysis was obtained from the primary tumor of a 65 year-old male suffered from stage 4 oral squamous cell carcinoma. Tissue sections prepare were follow by Visium Spatial Tissue Optimization User Guide Rev D (10x Genomics, CG000239). In brief, frozen samples were cryosectioned on Visium Tissue Optimization Slides. Histology images were taken using Olympus IX83 (10X PH Objective). Library construction was according to the Visium Spatial Gene Expression User Guide. Libraries were loaded at 250 pM and sequenced on a NovaSeq 6000 System (Illumina) using a NovaSeq S4 Reagent Kit (300 cycles, 20012866, Illumina), at a sequencing depth followed the formula provided by the

manufacturer (10X Genomics): Calculate total sequencing depth  $\geq$  coverage area x total spots on the capture area x 50000 read pairs/ spots. (Coverage area: 20.8%, 36.1%, 26.8%, 31.5% / Sequencing depth: 96M, 170M, 126M, 146M read pairs) Data processing of Visium data, raw FASTQ files and images were output with Space Ranger software (Version 1.2.1), hg38 reference genome was used for gene alignment. Analyzing of gene sets (inflammasome related genes and EMT genes) and visualization image were produced by Loupe Browser 5.1.0. Analyzing of gene sets of the inflammasome-related genes<sup>6</sup> and EMT genes<sup>4</sup>, and visualization image were produced by Loupe Browser 5.1.0.

### **Generation of the *MIR21/mir21* knockout cell line**

To generate *MIR21*-knockout THP1 (THP1<sup>*MIR21*<sup>-/-</sup></sup>) and *mir21*-knockout MTCQ1 (MTCQ1<sup>*mir21*<sup>-/-</sup></sup>) cells, the genomic region flanking *MIR21-5p* / *mir21a-5p* was deleted using the CRISPR/Cas9 system. Briefly, THP-1 or MTCQ1 cells were subjected to transfection with pSpCas9(BB)-2A-Puro (PX459) and pEGFP-N3 pSurrogate reporter, and the in-of-flam dTomato signal was sorted by using FACS Aria (BD). The exact deleted sequence of the *MIR21* / *mir21* genome was cloned using the TA Cloning™ Kit (Thermo) and confirmed by conducting direct sequencing (supplementary figure 4C and figure 4A). The depletion of miR-21/mir-21 in THP-1/MTCQ1 cells was confirmed by performing stem-loop reverse transcription-qPCR.

### **Quantitative RT-PCR**

Quantitative PCR was performed using the StepOnePlus real-time PCR system (Applied Biosystems Inc., Foster City, CA, USA). The primer sequences used for real-time PCR are listed in supplementary table 14.

### **Immunoblotting and immunoprecipitation**

These procedures were performed as per previously described protocols<sup>4</sup>. The results were measured using the GE LAS-4000 biomolecular imager (GE Healthcare Inc., Marlborough, MA). The information on antibodies

used in the experiments is listed in supplementary table 14.

### **Immunohistochemistry (IHC)**

The paraffin-embedded tissue sections were subjected to deparaffinization and retrieval, followed by subsection to washing steps with water and blockade with 3% hydrogen peroxide. The samples were washed first with water and subsequently with PBS, after which they were subjected to blockade and stained with antibodies, and were subsequently subjected to enzymatic avidin-biotin complex (ABC)-diaminobenzidine (DAB) staining (Leica Biosystems, Wetzlar, Germany). Nuclei were subjected to counterstaining with haematoxylin. All comparative images were obtained using an identical microscope and camera settings (Olympus BX51; Olympus Corporation, Tokyo, Japan). For scoring the Snail expression by IHC, ten high-power field images were taken from each sample and interpreted by two independent observers. The mean value of the percentage of nuclear Snail-positive cancer cells was calculated and the Snail IHC score was defined as negative, less than 20% of cancer cells with nucleus staining; +, 20-50% of cancer cells with nucleus staining; and ++, >50% of cancer cells with nucleus staining. The information on the antibodies used in the experiments is listed in supplementary table 14.

### **Multiplex immunofluorescence staining of HNSCC samples**

To perform staining of multiple markers, namely CD4, CD8a, CD163, CD68, CD66b, and PanCK, via multiplex immunofluorescence staining, samples were stained using the Opal 7-Color IHC Kit (Akoya Biosciences) and the corresponding antibodies. After the performance of staining, the Vectra Polaris Automated Quantitative Pathology Imaging System (Akoya Biosciences) was used to scan multispectral data using the Form Tissue Analysis Software (Akoya Biosciences). ImageJ was used to unmix the overlapping signals and to measure the positive signal of each slide. A total of nine patients and ten multispectral images from each patient were involved and analyzed. The information on the antibodies used in the experiments is listed in supplementary table 14.

### Proximity ligation assay

The proximity ligation assay (PLA) was performed to investigate the proximity of epitopes recognized by the anti-NLRP3 and anti-ASC antibodies, representing the assembly of NLRP3 inflammasomes in macrophages. Briefly, after incubation with primary antibodies, DuoLink® In Situ PLA probes (Merck KGaA, Burlington, MA) were used and incubation was performed for 1 h at 37°C. Subsequent ligation and detection were performed using the DuoLink® In Situ Detection Reagents Red Kit (Merck KGaA, Burlington, MA, USA). Blockade, antibody hybridization, proximity ligation, and detection were performed according to the manufacturer's recommendations. The fluorescence images were captured using the Olympus Fluoview FV10i Laser confocal microscope (Olympus Corporation, Tokyo, Japan) equipped with a 60x oil objective (Olympus UPLSAPO 60XO, NA 1.35) and analyzed using Olympus FV10-ASW Version 3.0. The PLA signal was quantified by measuring the number of red dots per cell. The total number of quantified cells from randomly selected fields is detailed in the corresponding figure legends.

### Luciferase reporter assay

For conducting the *BRCC3* 3'-UTR reporter assay, 50 ng of the wild-type or mutated reporter constructs (+985 to +1784 of the transcription start site TSS), 100 ng of a pCMV-β-gal internal control plasmid, and 3 μg of pCDNA3-miR21 or control vector were co-transfected into HEK-293T cells. Luciferase activity was measured after 48 h of incubation.

### SYTOX Green assay

The SYTOX Green staining was applied to assay the pyroptotic cells. THP-1 WT or THP-1<sup>MIR21<sup>-/-</sup></sup> were differentiated with PMA (20 ng/ml) and 5 × 10<sup>5</sup> cells were seeded onto dishes overnight. NLRP3 inflammasome activation was induced by LPS (1 μg/ml) for 4 hours followed by nigericin (5 μM) for 1 hour, then the cell was incubated with RPMI containing SYTOX green (1 μM, S7020, Thermo Fisher Scientific). Cells were measured

by microplate reader for Ex 488 nm and Em 513 nm.

### Animal experiments

C57BL/6J and BALB/c mice (6 to 8 weeks old) were purchased from the National Laboratory Animal Center (Taipei, Taiwan) and were housed in a pathogen-free environment (50% humidity and 22 °C). All animals and experiments were conducted by the Institutional Animal Care and Use Committee of National Yang Ming Chiao Tung University and Taipei Veterans General Hospital with approval IDs (IACUC certificate No. 1090514 of National Yang Ming Chiao Tung University and IACUC certificate No. 2013-169 of Taipei Veterans General Hospital). All mice were acclimated for 3 to 7 days before the experiment. Mice were randomized into different experimental groups. Tumor size was measured and recorded using a digital caliper.

The *in vivo* caspase activity assay (figure 4B,C), tumor measurement (figure 4D-F), and single-cell RNA-sequencing analysis (figure 6, supplementary figure 8, supplementary figure 9) were performed using the MTCQ1-C57BL/6J syngeneic murine oral squamous cell carcinoma model<sup>7</sup>. For the *in vivo* caspase-1 activity assay,  $1 \times 10^6$  MTCQ1-WT or MTCQ1<sup>mir21-/-</sup> cells were inoculated into the subcutaneous region of the wild-type C57BL/6 mice for 14 days. The mice received intraperitoneal injection of cisplatin (5 mg/kg/day) or phosphate-buffered saline (PBS) since the 14<sup>th</sup> day for 4 consecutive days. Mice were sacrificed on the 19<sup>th</sup> day. The tumor specimens were collected, and the F4/80<sup>+</sup> TAMs were isolated to determine caspase 1 activity (F4/80<sup>+</sup> FLICA<sup>+</sup> cells, ImmunoChemistry Technologies, Davis, CA). To measure the size and weight of the tumors,  $1 \times 10^6$  MTCQ1-WT or MTCQ1<sup>mir21-/-</sup> cells were inoculated into the subcutaneous region of wild-type or *Nlrp3*<sup>-/-</sup> C57BL/6J mice. The developed tumors were measured regularly and allowed to grow until the average volume reached 50 mm<sup>3</sup> (volume = width<sup>2</sup> × length/2). Mice received PBS or 5 mg/kg cisplatin daily every 3 days for a total of six doses. The mice were sacrificed on the 18<sup>th</sup> day, and the weights of the tumors were recorded. For single-cell RNA-sequencing (scRNA-seq) analysis,  $1 \times 10^6$  MTCQ1-WT or MTCQ1<sup>mir21-/-</sup> cells were injected into the subcutaneous region of the wild-type C57BL/6J mice for 14 days (n=3 for each group). Intraperitoneal injection of cisplatin 5 mg/kg was administered on the 14<sup>th</sup> day, and the tumors were harvested



for scRNA-seq analysis.

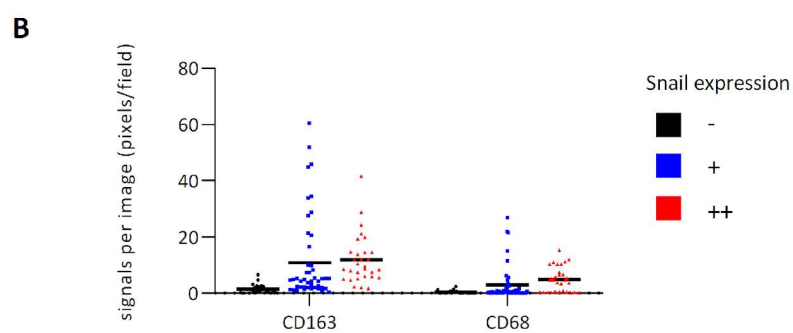
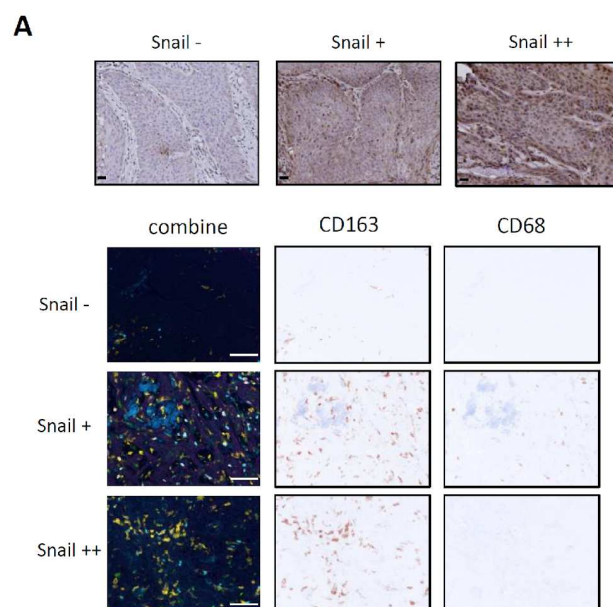
We applied two additional syngeneic murine tumor models, 4T1-BALB/c and LLC-C57BL6/J in the study. *In vivo* PLA and serum IL-1 $\beta$  levels were detected in both syngeneic models (figure 5A-E, supplementary figure 7). Tumor size and weight were measured, and the infiltrated T cells were analyzed in the LLC-C57BL6/J model (figure 5F-I). For *in vivo* PLA in the 4T1-BALB/c model (figure 5A-B),  $2.5 \times 10^5$  tumor cells were intravenously injected into the tail veins of the mice. The tumor-bearing mice received a single injection of 5 mg/kg cisplatin on the 14<sup>th</sup> day after tumor-cell injection. The mice were euthanized on the 17<sup>th</sup> day after the tumor cell injection. F4/80<sup>+</sup> macrophages were isolated from the lungs, and PLA was performed using these cells. For measuring serum IL-1 $\beta$  levels to represent inflammasome activities in the 4T1-BALB/c model (supplementary figure 7B), a total of  $5 \times 10^5$  4T1 cells expressing Snail or a control vector were injected into the mammary fat pad of BALB/c mice. The tumor-bearing mice received a single intraperitoneal injection of cisplatin (5 mg/kg body weight) on the 10<sup>th</sup> day after tumor-cell injection. The mice were euthanized on the 13<sup>th</sup> day after the tumor cell inoculation. The sera were harvested and IL-1 $\beta$  levels were detected using a mouse IL-1 $\beta$  ELISA kit. For assaying the viability of tumor-associated macrophages (supplementary figure 7A),  $1 \times 10^6$  MTCQ1-WT or MTCQ1<sup>mir21<sup>-/-</sup></sup> cells were inoculated into the subcutaneous region of wild-type C57BL/6 mice for 14 days. Mice received intraperitoneal injection of cisplatin (5 mg/kg/day) or PBS since the 14<sup>th</sup> day for 4 consecutive days. The mice were sacrificed on day 19. The tumor specimens were collected and then stained with 7-aminoactinomycin D (7-AAD) solution (5  $\mu$ L in 400  $\mu$ L cell sample, Abcam, Cambridge, UK) before analysis. The CD11b<sup>+</sup>F4/80<sup>+</sup>7AAD<sup>+</sup> TAMs were determined by flow cytometry. For examining PLA and serum IL-1 $\beta$  levels in the LLC-C57BL/6 model (figure 5C),  $5 \times 10^5$  LLC1 cells transfected with shRNA against murine Snail or a control sequence were inoculated into the subcutaneous area wild-type or *Nlrp3<sup>-/-</sup>* C57BL/6J mice. The tumor-bearing mice received a single intraperitoneal injection of 5 mg/kg cisplatin on the 10<sup>th</sup> day after tumor cell injection. The mice were euthanized on the 13<sup>th</sup> day after the tumor cell inoculation. The tumors were harvested for PLA and sera were harvested for examining IL-1 $\beta$  levels. To measure the tumor size in the LLC-C57BL/6 model (figure 5F-G),  $5 \times 10^5$  LLC cells receiving shRNA against Snail or a control sequence

were injected into the subcutaneous region of the wild-type or *Nlrp3*<sup>-/-</sup> C57BL/6J mice. The developed tumors were measured regularly and allowed to grow until the average volume reached 50 mm<sup>3</sup>. Mice received PBS or 5 mg/kg/day for 4 consecutive days for a total of four doses. The mice were sacrificed on the 16<sup>th</sup> day, and the weights of the tumors were recorded. For quantification of CD8<sup>+</sup>IFN- $\gamma$ <sup>+</sup> T-cell infiltration and *Ifgr* expression in tumors (figure 5H-I), wild-type C57BL/6 mice were inoculated subcutaneously with  $2.5 \times 10^5$  LLC-Ctrl or LLC-shSnail cells. The developed tumors were measured regularly and allowed to grow until the average volume reached 50 mm<sup>3</sup>. Mice received PBS or 5 mg/kg cisplatin daily for four consecutive days in the LLC1 model. The mice were euthanized on the 16<sup>th</sup> day post-cisplatin injection. The tumor-infiltrating CD8<sup>+</sup> IFN- $\gamma$ <sup>+</sup> T cells were analyzed using flow cytometry. The expression of *Ifgr* in tumors was examined using RT-qPCR (figure 5I).

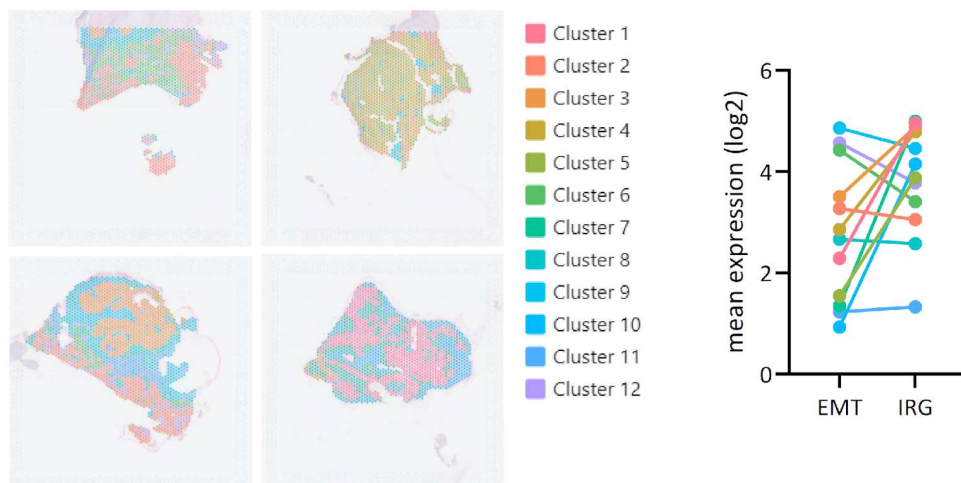
## References

1. Eisenhauer EA, Therasse P, Bogaerts J, Schwartz LH, Sargent D, Ford R, *et al.* New response evaluation criteria in solid tumours: revised RECIST guideline (version 1.1). *Eur J Cancer* **2009**;45:228-47.
2. Goldman MJ, Craft B, Hastie M, Repecka K, McDade F, Kamath A, *et al.* Visualizing and interpreting cancer genomics data via the Xena platform. *Nat Biotechnol* **2020**;38:675-8.
3. Cerami E, Gao J, Dogrusoz U, Gross BE, Sumer SO, Aksoy BA, *et al.* The cBio cancer genomics portal: an open platform for exploring multidimensional cancer genomics data. *Cancer Discov* **2012**;2:401-4.
4. Chae YK, Chang S, Ko T, Anker J, Agte S, Iams W, *et al.* Epithelial-mesenchymal transition (EMT) signature is inversely associated with T-cell infiltration in non-small cell lung cancer (NSCLC). *Sci Rep* **2018**;8:2918.
5. Hsieh CH, Tai SK, Yang MH. Snail-overexpressing cancer cells promote M2-Like polarization of tumor-associated macrophages by delivering miR-21-abundant exosomes. *Neoplasia* **2018**;20:775-88.
6. Zheng T, Wang X, Yue P, Han T,
7. Hu Y, Wang B, *et al.* Prognostic inflammasome-related signature construction in kidney renal clear cell carcinoma based on a pan-cancer landscape. *Evid Based Complement Alternat Med* **2020**;2020:3259795.
8. Chen YF, Chang KW, Yang IT, Tu HF, Lin SC. Establishment of syngeneic murine model for oral cancer therapy. *Oral Oncol* **2019**;95:194-201.

## Supplementary Figures

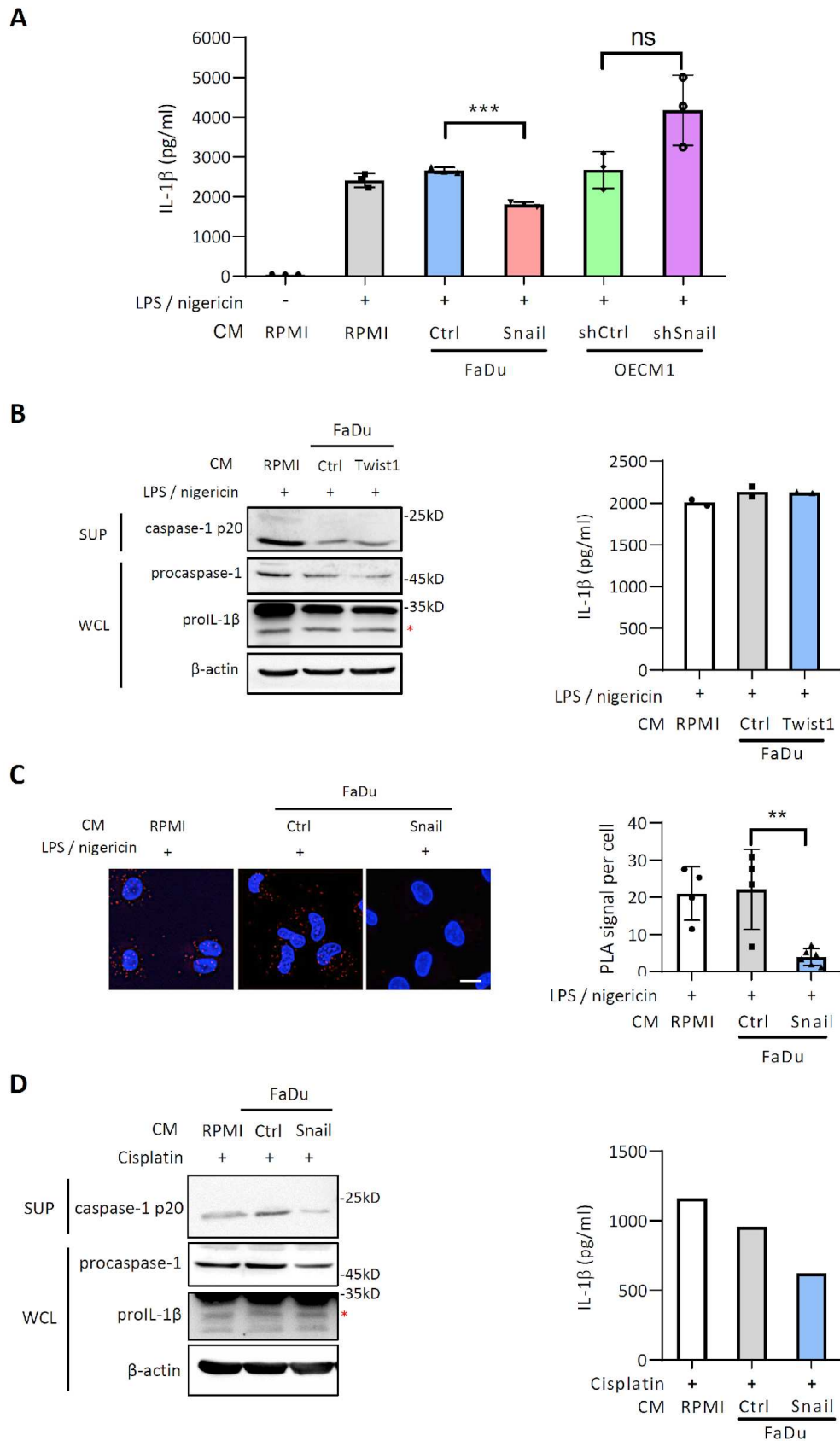


**C**



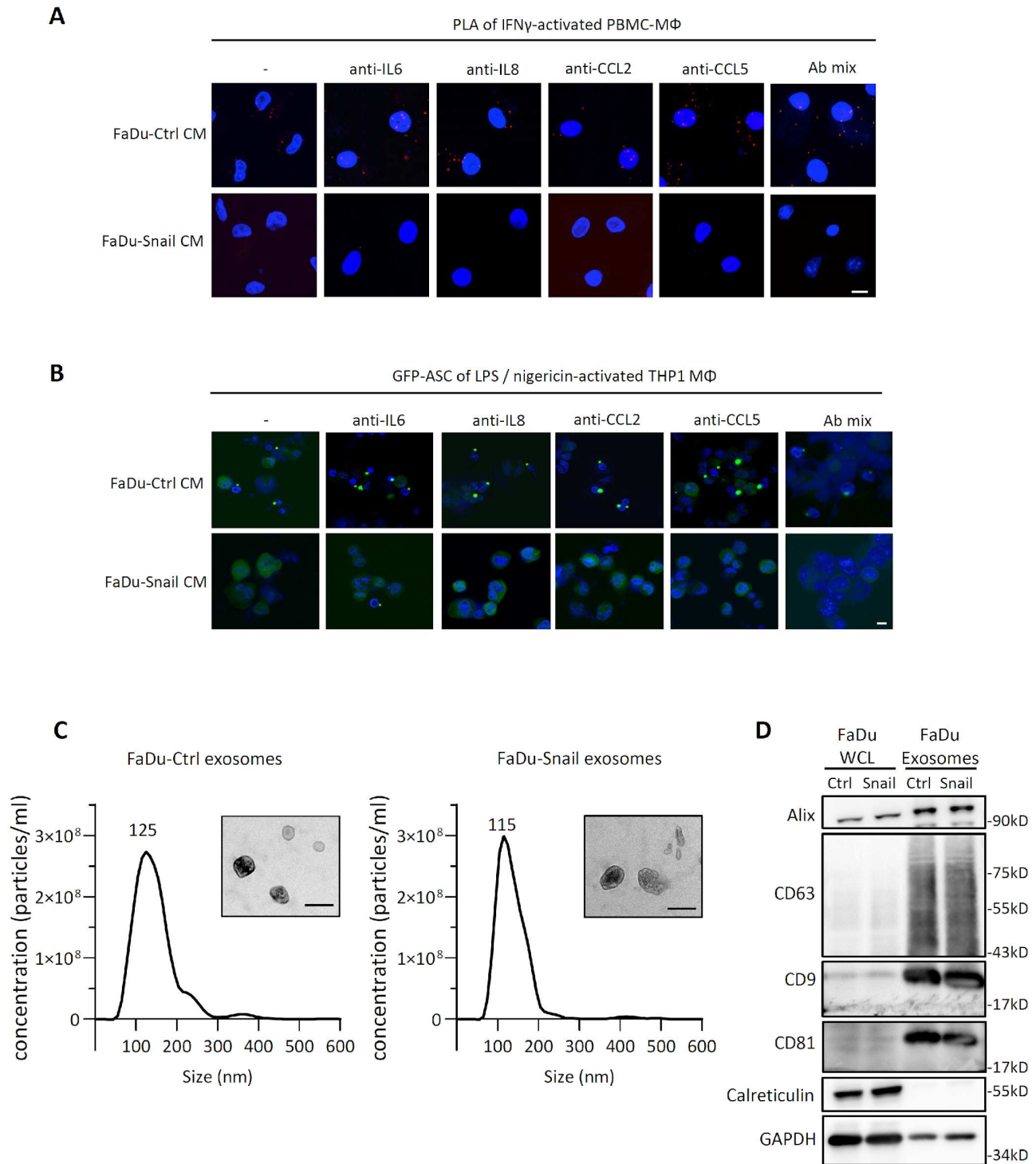
**Supplementary figure 1. EMT is associated with the immunosuppressive microenvironments.**

- (A) Multiplex immunofluorescent staining in 9 HNSCC samples with differential expression levels of Snail (three cases for each expression level). Upper, representative IHC of Snail. Lower, representative images of multiplex immunofluorescent staining of different markers in Snail (-, +, ++) cases.
- (B) Quantification of the percentage of CD68 and CD163 signals in each image. Each group contains 3 patients and each patient contains 10 randomly selected fields were quantified for the signals. Scale bar=100  $\mu$ m.
- (C) Visium spatial transcriptomic analysis of a HNSCC tumor sample. Left, distribution of 12 transcriptomic clusters in the tumor sample. Right, the expression of EMT-related gene and inflammasome-related genes in the 12 clusters. The gene list of the EMT-related genes and inflammasome related genes is shown in supplementary table 3. IRG, inflammasome-related genes.



**Supplementary figure 2. The supernatants of Snail-expressing cancer cells inhibit activation of NLRP3 inflammasomes.**

- (A) ELISA for analyzing the level of secreted IL-1 $\beta$  by LPS/nigericin-activated THP1-derived macrophages incubated with the conditioned media (CM) from FaDu-Ctrl versus FaDu-Snail and OECM1-Ctrl versus OECM1-shSnail. RPMI group was used as a baseline control of ELISA. Data shows mean  $\pm$  S.D., n=3 independent experiment (each experiment contains 2 technical replicates). \*\*\* $P < 0.001$ , ns= no significance by Student's t-test.
- (B) Left, immunoblots of cleaved caspase-1 p20 in supernatants (SUP), pro-caspase-1 and pro-IL-1 $\beta$  in whole cell lysates (WCL) of LPS/nigericin-activated THP1-derived macrophages incubated with the conditioned media (CM) from FaDu-Ctrl versus FaDu-Twist1 for 24 hr.  $\beta$ -actin was used as a loading control for immunoblots. Right, ELISA for analyzing the level of secreted IL-1 $\beta$  by activated THP1-derived macrophages in the corresponding groups. Data represent means  $\pm$  S.D. n=2 independent experiment (each experiment contains 2 technical replicates).
- (C) Left, proximity ligation assay (PLA) signal of NLRP3 and ASC interaction in LPS/nigericin-stimulated PBMC-derived macrophages incubate with conditioned media from FaDu-Vec or FaDu-Snail. Nigericin was used for inflammasome activation. Scale bar, 10  $\mu$ m. Right, quantification of number of PLA signals per cell. For each group, at least a total of fifteen cells from five randomly selected fields (four for FaDu-Ctrl) were used for PLA quantification. Data represent means  $\pm$  S.D. \*\* $P < 0.01$  by Student's t-test.
- (D) Left, immunoblots of cleaved caspase-1 p20 in supernatants (SUP), pro-caspase-1 and pro-IL-1 $\beta$  in whole cell lysates (WCL) of cisplatin-activated PBMC-derived macrophages incubated with conditioned media from FaDu-Ctrl/FaDu-Snail.  $\beta$ -actin was used as a loading control for immunoblots. Right, ELISA for analyzing the level of secreted IL-1 $\beta$  by cisplatin-activated macrophages. The data is derived from one independent experiment with 2 technical replicates.

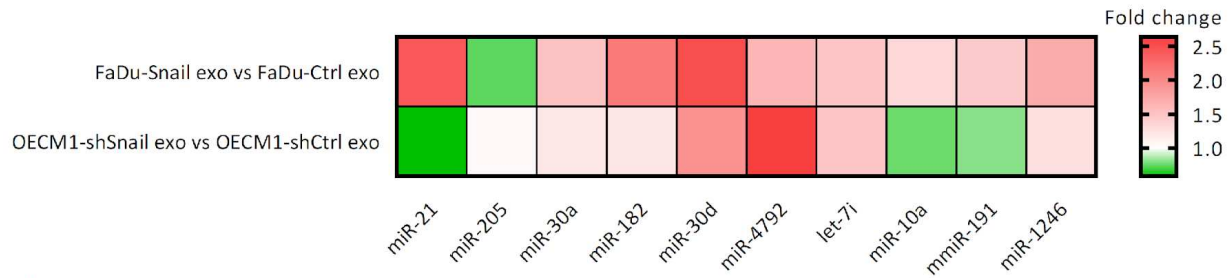


**Supplementary figure 3. Snail-expressing cancer cells suppress inflammasome activation and characterization of exosomes secreted by cancer cells.**

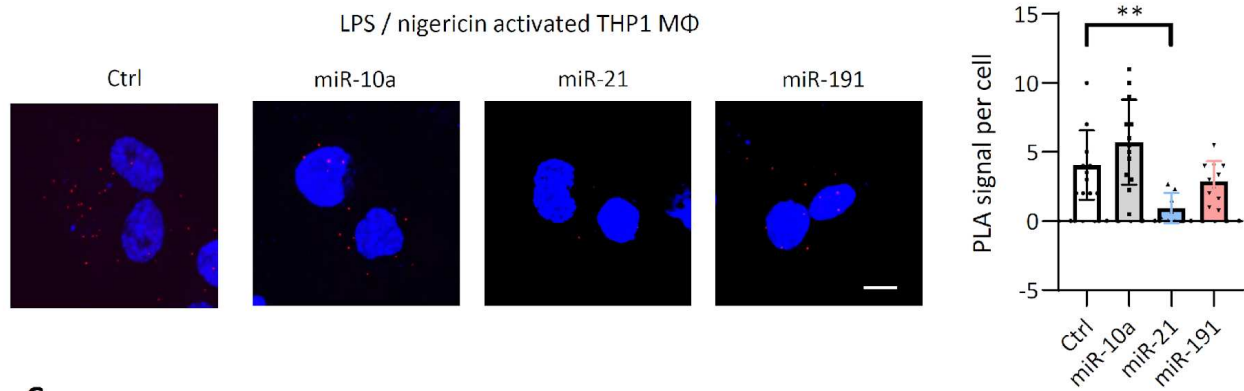
- (A) PLA for detecting NLRP3 and ASC interaction in IFN- $\gamma$ -activated PBMC-derived macrophages in conditioned media from FaDu-Ctrl/FaDu-Snail in the presence of neutralizing antibodies as indicated (anti-IL6, antiIL-8, anti-CCL2, anti-CCL5, mix) for 24 h (0.5  $\mu$ g/ml). Scale bar, 10  $\mu$ m.
- (B) Immunofluorescent images of LPS/nigericin-activated THP1-derived macrophages transfected with GFP-tagged ASC and incubated with conditioned media from FaDu-Ctrl/FaDu-Snail in the presence of indicated neutralizing antibodies (anti-IL6, antiIL-8, anti-CCL2, anti-CCL5, mix) for 24 h. Scale bar, 10  $\mu$ m.
- (C) Characterization of exosomes from FaDu-Ctrl/FaDu-Snail by nanoparticle tracking analysis (NTA) and transmission electron microscopy (TEM). The insets show the representative images of TEM. Scale bar=100 nm.
- (D) Western blots for analyzing the expression of Alix, CD63, CD81, CD9, and calreticulin for exosomes and whole cell lysate (WCL) from FaDu-Ctrl/ FaDu-Snail. GAPDH was a loading control.



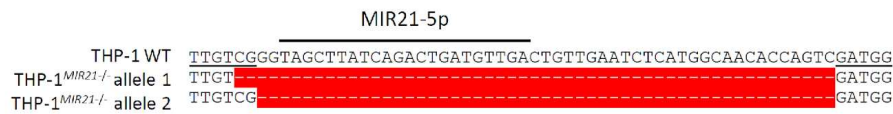
**A**



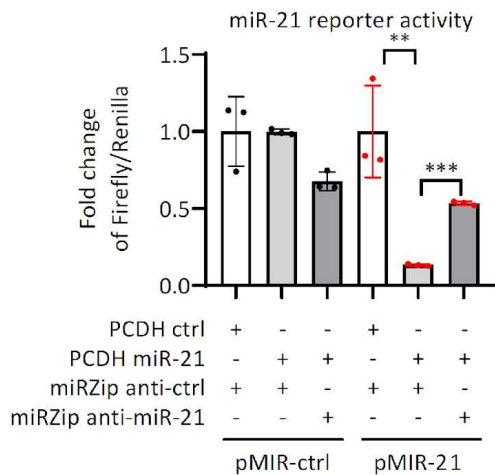
**B**



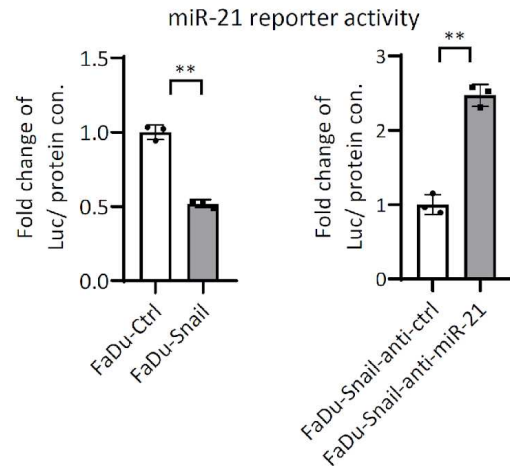
**C**



**D**

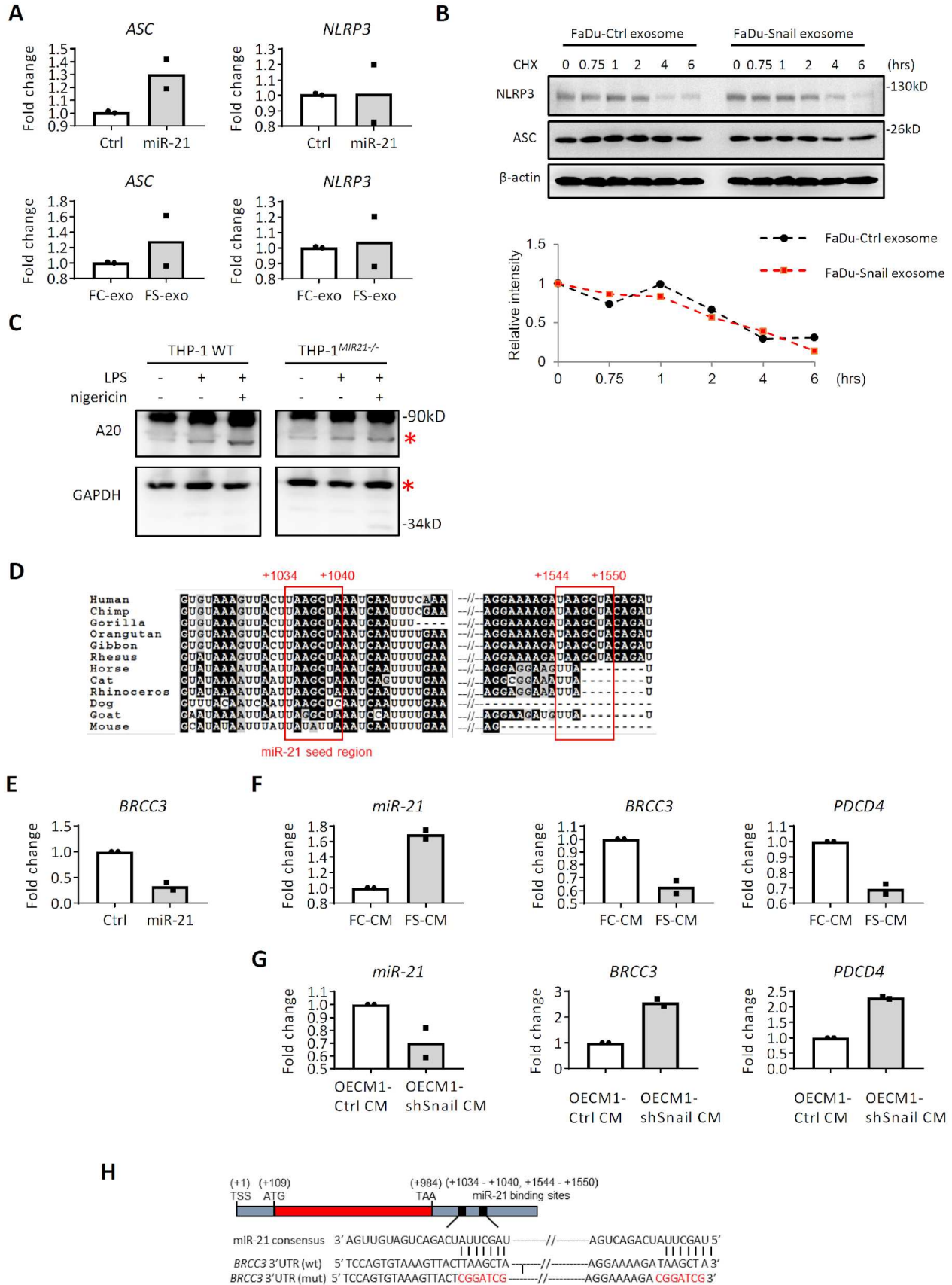


**E**



**Supplementary figure 4. Snail-expressing cancer cells secrete miR-21-abundant exosomes and miR-21 suppress NLRP3 inflammasome activities.**

- (A) RT-qPCR for analyzing the exosomal miRNAs derived from FaDu-Ctrl/FaDu-Snail and OECM1-Ctrl/OECM1-shSnail. The selected miRNAs were ranked top 10 in oral cancer-derived exosomes (from exosomal RNA-seq, see Supplementary Table S6). Red, upregulation; green, downregulation. The data is derived from one independent experiment with 2 technical replicates.
- (B) Left, representative images of PLA for detecting NLRP3 and ASC interaction in LPS/nigericin-activated THP-1- derived macrophages transfected with miR-10a, miR-21, miR191, or a control agomir. Scale bar, 10  $\mu$ m. Right, quantification of number of PLA signals per cell. For each group, at least a total of nineteen cells from randomly selected fields were used for PLA quantification. Data represent means  $\pm$  S.D. **\*\* $P < 0.01$**  by Student's *t*-test.
- (C) Left, genomic sequence of *MIR-21* region of the wild-type THP-1 cell line (THP1-WT) or receiving CRISPR/Cas9 to knock out *MIR21* (THP1<sup>MIR21<sup>-/-</sup></sup>). Right, RT-qPCR for detecting the expression level of expression in THP1-WT and THP1<sup>MIR21<sup>-/-</sup></sup>. n=3 independent experiments (each contains 2 technical replicates). Data shows mean  $\pm$  S.D. **\*\* $P < 0.01$**  by Student's *t*-test.
- (D) A reporter assay for confirming the activity of miRZip anti-miR-21. HEK-293T cells were transfected with the indicated plasmids and the fold change of firefly/renilla luciferase ratio was calculated to represent the relative reporter activity of each condition. Data represent means  $\pm$  S.D. n=3 independent experiment (each experiment contains 2 technical replicates). **\*\* $P < 0.01$** , **\*\*\* $P < 0.001$**  by Student's *t*-test.
- (E) A reporter assay for confirming the activity of anti-miR-21 in FaDu-ctrl/FaDu-Snail (left) and FaDu-Snail transfected with anti-miR-21/control sequence (right). Data represent means  $\pm$  S.D. n=3 independent experiment (each experiment contains 2 technical replicates). **\*\* $P < 0.01$**  by Student's *t*-test.

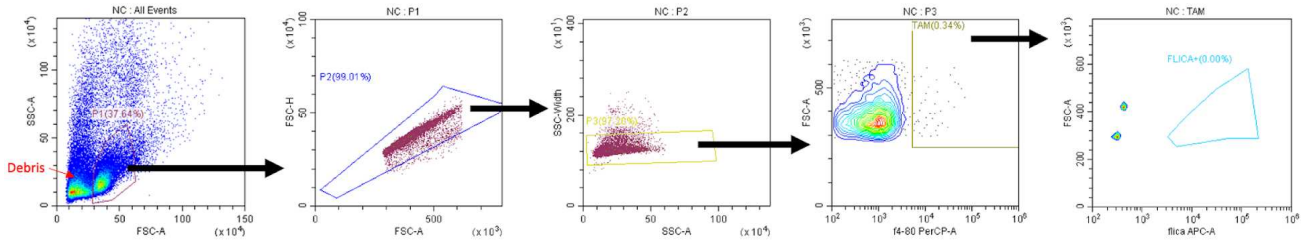


**Supplementary figure 5. miR-21 targets the 3'-UTR region of *BRCC3* to suppress its expression.**

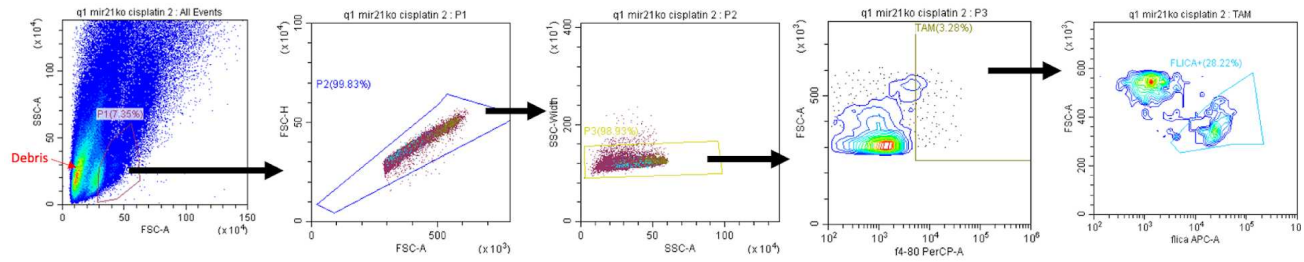
- (A) RT-qPCR for analyzing the expression of ASC and NLRP3 in IFN $\gamma$ -activated PBMC-derived macrophages transfected with miR-21 or control agomir (upper panels), or macrophages incubated with exosomes from FaDu-Ctrl or FaDu-Snail (FC-exo/FS-exo; upper panels). n=2 independent experiments (each experiment contains 2 technical replicates).
- (B) Upper, western blot of NLRP3 and ASC in IFN $\gamma$ -activated PBMC-derived macrophages incubated with exosomes derived from FaDu-Ctrl or FaDu-Snail in the presence of cycloheximide (CHX) to inhibit de novo protein synthesis. Lower, relative intensity of NLRP3 protein expression.
- (C) Western blot of A20 in macrophages derived from wild-type THP1 (THP1-WT) or miR-21 knockout THP1 (THP1<sup>MIR21<sup>-/-</sup></sup>). LPS and nigericin were applied for inflammasome activation. GAPDH was a loading control.
- (D) Alignment of the sequences of miR-21 seed regions in *BRCC3* 3'-UTR among different species.
- (E) RT-qPCR of *BRCC3* in IFN $\gamma$ -activated PBMC-derived macrophages transfected with miR-21 or control agomir. Data represent means  $\pm$  S.D. n=2 independent experiments (each experiment contains 2 technical replicates).
- (F) RT-qPCR of miR-21, *BRCC3*, and *PDCD4* in IFN $\gamma$ -activated PBMC-derived macrophages incubated with conditioned media (CM) from FaDu-Ctrl(FC)/FaDu-Snail(FS) for 48 h. n=2 independent experiments (each experiment contains 2 technical replicates).
- (G) RT-qPCR of miR-21, *BRCC3*, and *PDCD4* in IFN $\gamma$ -activated PBMC-derived macrophages incubated with conditioned media (CM) from OECM1-Ctrl/OECM1-shSnail for 48 h. n=2 independent experiments (each experiment contains 2 technical replicates).
- (H) Representation of the organization of *BRCC3* transcript, and the wild-type or miR-21 binding site mutated 3'-UTR reporter constructs of *BRCC3* (pMIR-*BRCC3*-wt and pMIR-*BRCC3*-mut).

**A**

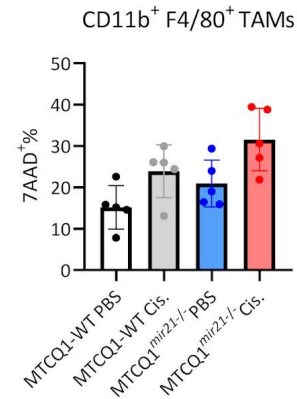
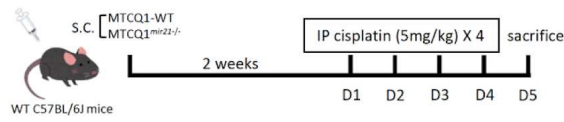
**Negative control (no stain)**



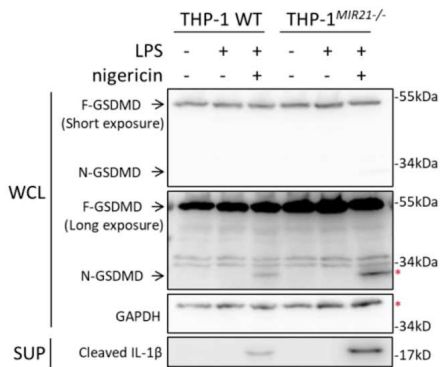
**Staining sample**



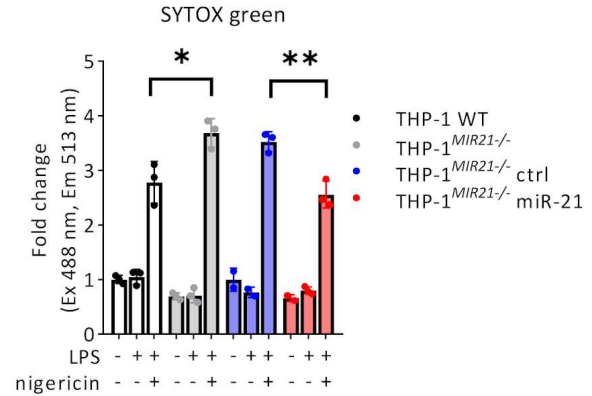
**B**



**C**



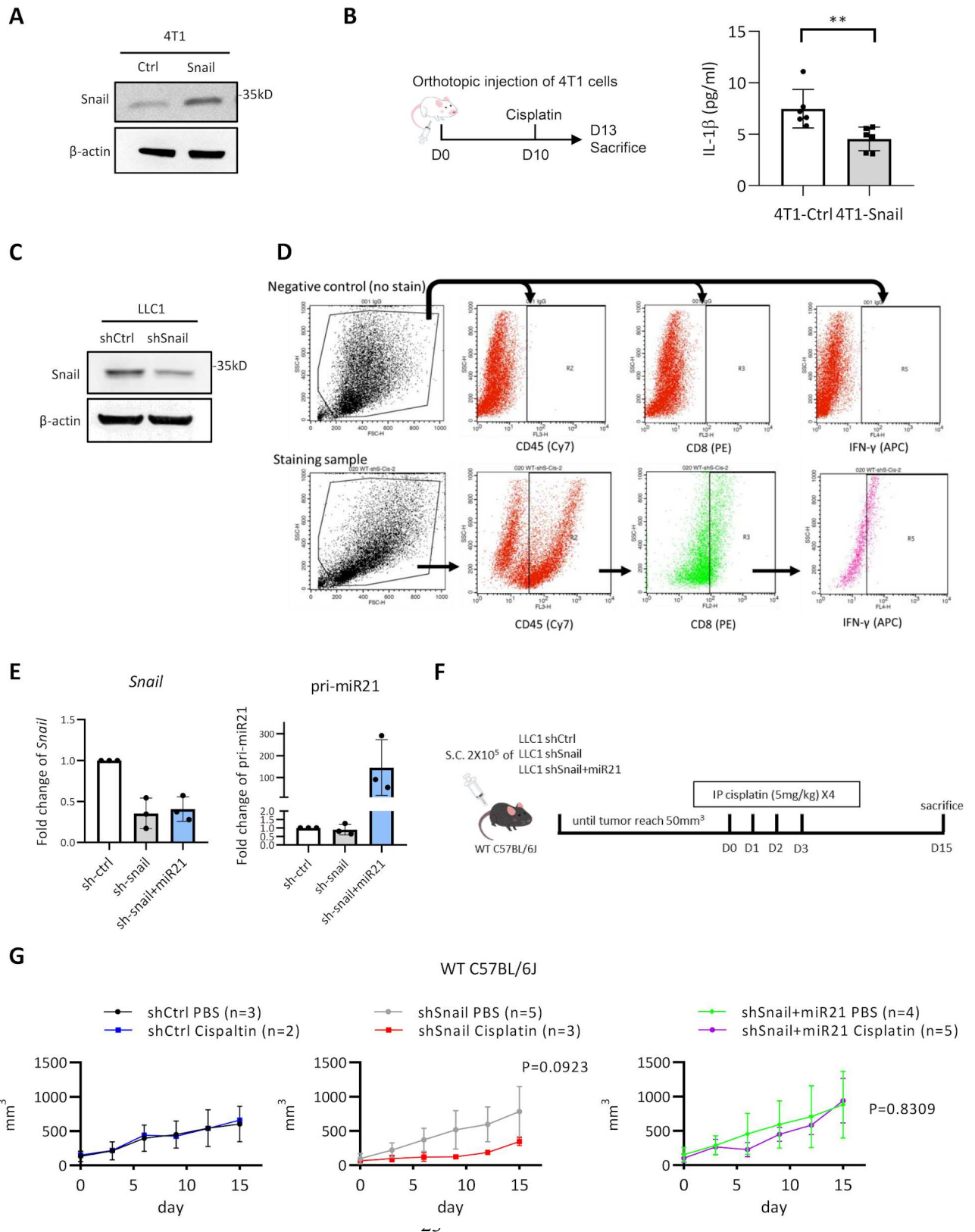
**D**



**Supplementary figure 6. The influence of miR-21 on the viability and pyroptosis of macrophages.**

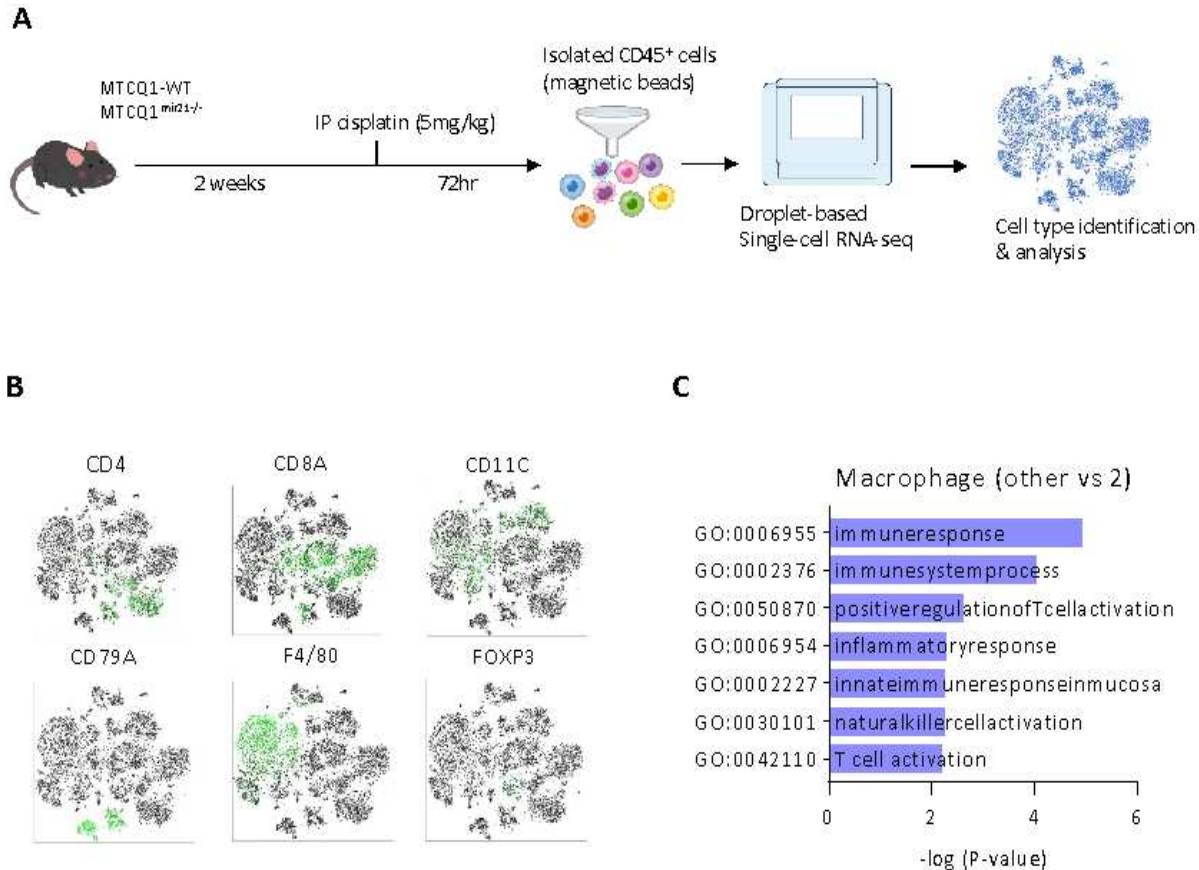
- (A) Representing results to show the gating strategy of caspase 1-activated F4/80<sup>+</sup> tumor-associated macrophages detected by FLICA staining in the experiment of figure 4C.
- (B) 7-aminoactinomycin D (7-AAD) staining for examination of the viability of tumor-associated macrophages (TAMs) from murine MTCQ1-WT/MTCQ1<sup>mir21<sup>-/-</sup></sup> cells-formed tumors. CD11b<sup>+</sup>F4/80<sup>+</sup> TAMs were sorted from the tumors for subsequent analysis. Left, schema of the animal experiment. Right, the percentage of 7-AAD<sup>+</sup> TAMs from MTCQ1-WT/MTCQ1<sup>mir21<sup>-/-</sup></sup> -formed tumors with or without cisplatin treatment. n=5 for each group. No statistical significance was reached in each comparison.
- (C) Western blots of full length gasdermin D (F-GSDMD), N-terminal gasdermin D (N-GSDMD) of whole cell lysates (WCL) and cleaved IL-1 $\beta$  of supernatant (SUP) from wild-type THP1 (THP1-WT) or miR-21 knockout THP1 (THP1<sup>MIR21<sup>-/-</sup></sup>) cells with or without LPS/nigericin treatment for inflammasome activation. GAPDH was a loading control.
- (D) SYTOX green assay. THP1-WT/THP1<sup>MIR21<sup>-/-</sup></sup> cells transfected with miR-21 or a control sequence were examined by SYTOX green staining. Inflammasome activation was induced by LPS and nigericin treatment. Cells were measured by microplate reader for Ex 488 nm and Em 513 nm. Data represent means  $\pm$  S.D. n=3 independent experiment (each experiment contains 2 technical replicates). \* $P$ <0.05, \*\* $P$ <0.01 by Student's  $t$ -test.





### Supplementary figure 7. The influence of Snail-mir21 axis on tumor-infiltrated immune cells and tumor growth.

- (A) Western blot of Snail in 4T1 cells transfected with Snail or a control vector (Ctrl).  $\beta$ -actin was a loading control.
- (B) Left, schema of the experiment. Orthotopic implantation of  $5 \times 10^5$  of 4T1-Ctrl or 4T1-Snail cells into the mammary fat pad of the BALB/c mice. Cisplatin (5 mg/kg) was given at 10<sup>th</sup> day after tumor cells inoculation. The mice were sacrificed at 13<sup>th</sup> day for analysis. Right, serum IL-1 $\beta$  level of mice at 13<sup>th</sup> day (n= 6). Data represent means  $\pm$  S.D. \*  $P < 0.01$  by Student's *t*-test.
- (C) Western blot of Snail in LLC1 cells receiving an shRNA against Snail (shSnail) or a control sequence (shCtrl).  $\beta$ -actin was used as a loading control.
- (D) Representing results to show the gating strategy of CD45<sup>+</sup>CD8<sup>+</sup>IFN $\gamma$ <sup>+</sup> T cells in the experiment of figure 5H.
- (E) RT-qPCR for examination of the expression of Snail and pri-miR21 in LLC cells expressed a shRNA against Snail (sh-Snail) or a control sequence (sh-ctrl), or sh-Snail and miR-21. Data represent means  $\pm$  S.D. n=3 independent experiment (each experiment contains 2 technical replicates).
- (F) Schema of the animal experiment in panel G.
- (G) Measurement of the volume of tumors formed by LLC1-shCtrl/LLC1-shSnail cells.  $2 \times 10^5$  cells were inoculated to the subcutaneous region of C57BL/6 mice. Cisplatin (5 mg/kg/day) were given for 4 continuous days since the tumor reached 50mm<sup>3</sup>. The mice were sacrificed at the 15<sup>th</sup> day after cisplatin/PBS treatment. Tumor volumes were recorded. Data (n>2) were presented in mean  $\pm$  S.D.

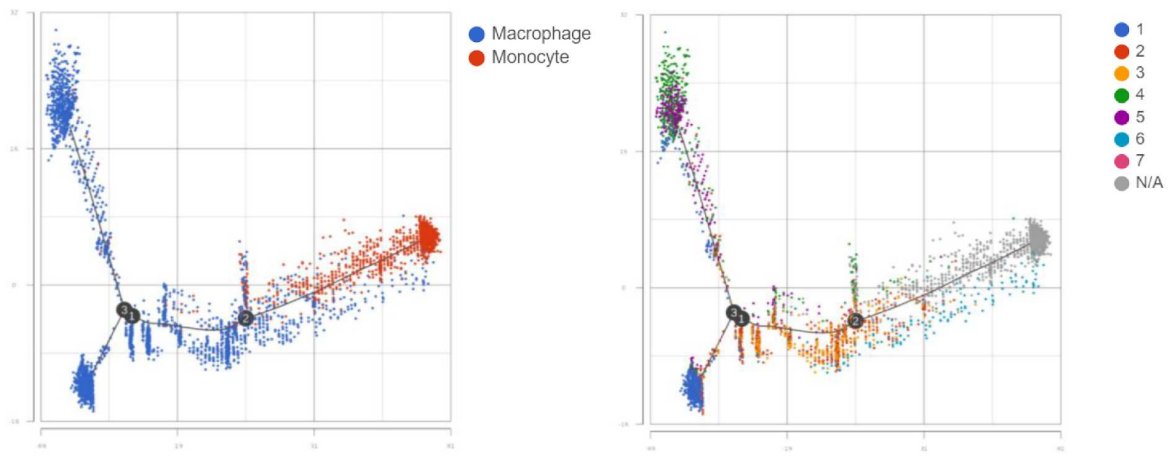




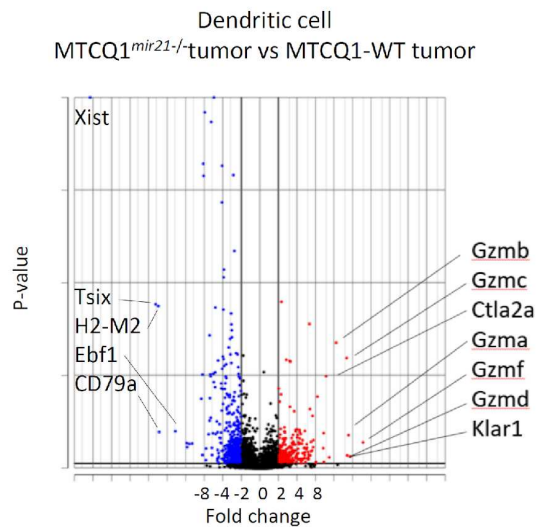
**Supplementary figure 8. Analysis of the infiltrated immune cells in murine oral cancers by single cell RNA sequencing.**

- (A) Schema of the experiment.  $1 \times 10^6$  MTCQ-WT/MTCQ<sup>mir21<sup>-/-</sup></sup> cells were inoculated to the subcutaneous region of the C57BL/6J mice for 2 weeks (n=3 for each group). Cisplatin 5mg/kg was given intraperitoneally on 14<sup>th</sup> day and the mice were sacrificed 72 h after cisplatin injection. The tumors were harvested and the CD45<sup>+</sup> cells were isolated by magnetic beads for the droplet-based single cell RNA sequencing and subsequent analysis.
- (B) t-SNE plots of the immune cells expressing different markers (CD4, CD8a, CD11c, CD79a, F4/80, and Foxp3) in MTCQ1-WT and MTCQ1<sup>mir21<sup>-/-</sup></sup>-formed tumors 3 days after cisplatin (5mg/kg) injection.
- (C) GO enrichment analysis of the biological pathways of the TAMs in other clusters versus cluster 2 (see Figure 6F for the TAM clustering).
- (D) A heatmap for showing the expression of the M1 macrophages-related genes (left) and M2 macrophages-related genes (right) in different clusters of macrophages. Red, upregulation; green, downregulation.

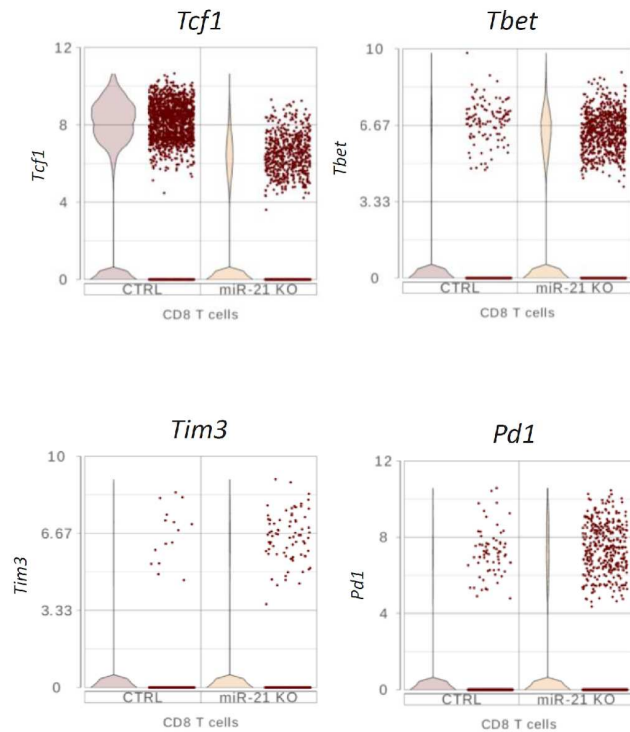
A



B

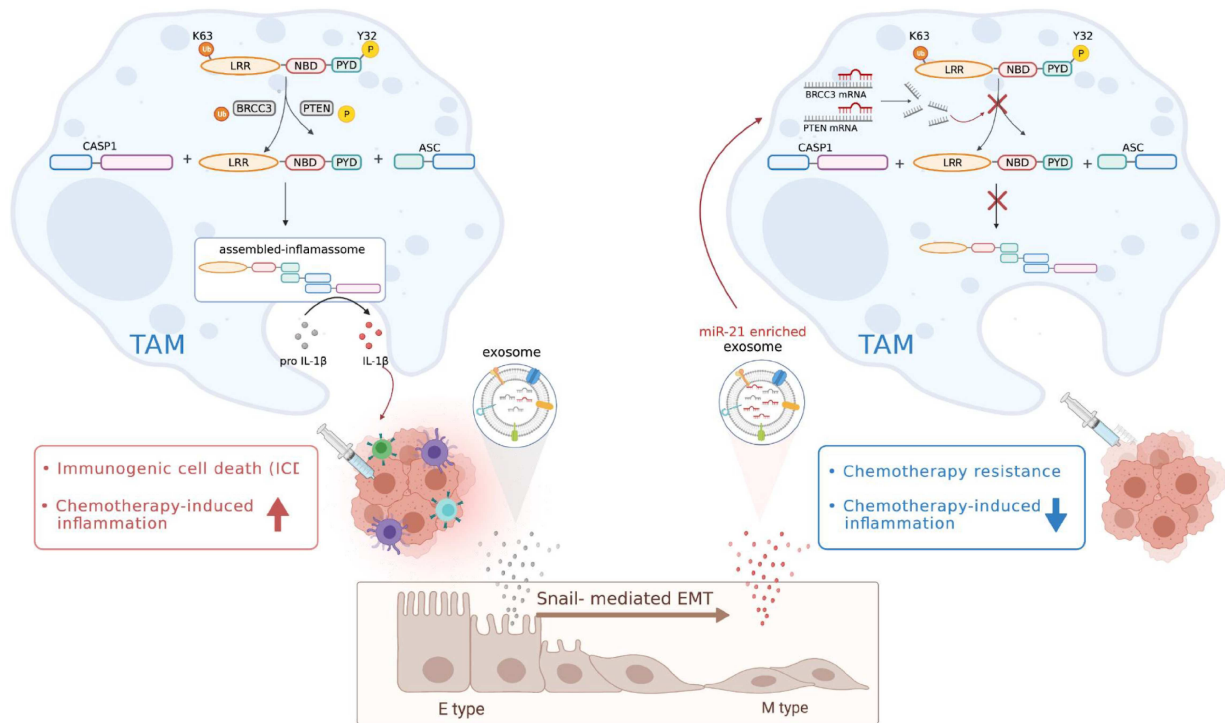


C



**Supplementary figure 9. Single cell RNA sequencing analysis of the infiltrated immune cells in murine oral cancers.**

- (A) Transcriptional trajectory of infiltrated macrophages and monocytes of the tumors.
- (B) Volcano plots of the differential expressed genes of the dendritic cells (classification by CIPR; see reference 28) from MTCQ<sup>mir21<sup>-/-</sup></sup>-versus MTCQ1-WT-formed tumors. Red, upregulated genes; blue, downregulated genes.
- (C) Violin plots to show the expression of the exhausted T cell markers (*Tcf1*, *Tbet*, *Tim3*, *Pd1*) in CD8<sup>+</sup> T cells of the MTCQ1-WT and MTCQ1<sup>mir21<sup>-/-</sup></sup> tumors.



**Supplementary figure 10.** The schema for representing the NLRP3 inflammasome activity of macrophages regulated by the Snail-miR-21 axis of cancer cells via exosomal delivery of miR-21. Created with [BioRender.com](https://www.biorender.com).

## Supplementary Table Legends

Supplementary Table 1. Characteristics of 9 TVGH HNSCC patients for multiplex immunofluorescent staining

Supplementary Table 2. Characteristics of the TVGH HNSCC patients for bulk RNA sequencing analysis (65 tumor tissues and 21 normal counterparts from 21 patients)

Supplementary Table 3. Characteristics of the TVGH HNSCC patients for RT-qPCR analysis (n=50)

Supplementary Table 4. Characteristics of the TVGH HNSCC patients for serum IL-1 $\beta$  analysis (n=19)

Supplementary Table 5. Characteristics of the TVGH HNSCC patients for immunofluorescent staining-PLA co-localization analysis (n=5)

Supplementary Table 6. List of the inflammasome-related genes and EMT genes for Visium spatial transcriptomic analysis

Supplementary Table 7. microRNA sequence profile in FaDu exosomes versus SG exosomes

Supplementary Table 8. Cell counts of different immune cells of the single cell RNA sequencing experiment

Supplementary Table 9. Differential gene expression of TAMs from MTCQ1-WT- vs. MTCQ1<sup>mir21<sup>-/-</sup></sup>-formed tumors

Supplementary Table 10. GO enrichment analysis of the TAMs from MTCQ1-WT- vs. MTCQ1<sup>mir21<sup>-/-</sup></sup>-formed tumors

Supplementary Table 11. Cell counts of macrophage subclusters of the single cell RNA sequencing experiment

Supplementary Table 12. GO enrichment analysis of the TAM subcluster 2 vs other TAM subclusters

Supplementary Table 13. Differential gene expression of dendritic cells MTCQ1-WT- vs. MTCQ1<sup>mir21<sup>-/-</sup></sup>-formed tumors

Supplementary Table 14. Antibodies, primers, plasmids, reagents, clinical samples, and other materials used in this study